Applied Surface Science 257 (2011) 6527–6530

Contents lists available at ScienceDirect

Applied Surface Science

journal homepage: www.elsevier.com/locate/apsusc

Synthesis of urchin-like Co_3O_4 hierarchical micro/nanostructures and their photocatalytic activity

Hui Li [a], Guang Tao Fei [a,*], Ming Fang [a], Ping Cui [a], Xiao Guo [a], Peng Yan [a,b], Li De Zhang [a]

[a] Key Laboratory of Materials Physics and Anhui Key Laboratory of Nanomaterials and Nanotechnology, Institute of Solid State Physics, Hefei Institutes of Physical Science, Chinese Academy of Sciences, PO Box 1129, Hefei 230031, People's Republic of China
[b] Binzhou Medical University, Binzhou, Shandong 256600, People's Republic of China

ARTICLE INFO

Article history:
Received 31 December 2010
Received in revised form 15 February 2011
Accepted 15 February 2011
Available online 24 February 2011

Keywords:
Co_3O_4
Urchin-like structure
Hydrothermal
Photocatalytic
Particle size

ABSTRACT

Urchin-like Co_3O_4 hierarchical micro/nanostructures have been successfully synthesized by calcining urchin-like precursor $CoCO_3$, which are prepared by a facile hydrothermal route. The particle size of the urchin-like Co_3O_4 could be easily controlled by altering the calcination temperature. The morphology and structure of the as-prepared urchin-like products were characterized by XRD, FESEM and TEM. Photocatalytic measurement demonstrates that these urchin-like Co_3O_4 micro/nanostructures show good photocatalytic effect and their degradation efficiency is strongly dependent on their particle size. Furthermore, a plausible reaction mechanism is also proposed to illustrate the photocatalytic processes of Co_3O_4.

1. Introduction

The ever-increasing demands for the textile promote the rapid development of the textile industries, but at the same time, it brings a large volume of waste water polluted by colored dyes [1]. As one of the most widely used ingredients for textile manufacturing, reactive dyes are toxic and non-biodegradable [2]. Therefore, many efforts have been devoted to remove these dyes from the waste water. Recently, the advanced oxidation processes (AOPs) have drawn much attention in the wastewater purification and other environment application [3–6]. Reactive species based AOPs are usually performed as effective photocatalytic medium through the photoexcitation of the semiconductors.

Co_3O_4, one of the most versatile transition-metal oxides, is widely applied in many fields, such as dyes degradation [7,8], gas sensors [9–11], lithium ion batteries [12–15], oxidation of CO at low temperature [16–18], and energy storage [19,20]. Rahman et al. [21] studied the synthesis of the Co_3O_4 nanoparticles by the hydrothermal process under the pulsed magnetic field and examined their electrochemical performances as an anode for the lithium ion battery. Askarinejad et al. [22] reported the catalytic performance of Co_3O_4 nanocrystals prepared by sonochemical method in epoxidation of styrene and cyclooctene. Patil et al. [23] reported the highly sensitive and fast responding sensor characteristics for CO of Co_3O_4 nanorods, which were obtained via the chemical co-precipitation/digestion methods.

Herein, we report the synthesis of the urchin-like precursor $CoCO_3$ through the facile and environment-friendly hydrothermal process, which subsequently transformed them to Co_3O_4 by calcination without change of its morphology. The as-synthesized Co_3O_4 hierarchical micro/nanostructure exhibits high degradation efficiency and superior stability for the reactive black dyes due to their large porosity and small particle size.

2. Experiment

2.1. Synthesis of Co_3O_4 nanocrystals

In our experiment, all chemicals were analytical grade and used without further purification. 1.50 g (25 mmol) of urea and 0.05 g of cetyltrimethylammonium bromide (CTAB) were dissolved in 30 ml deionized water under stirring. After the solution was transparent, 10 ml 0.5 M of $CoSO_4{\cdot}7H_2O$ were added and stirred for another 10 min. Finally, the whole mixture was transferred into a Teflon-lined autoclave and maintained at 120 °C for 12 h. When the autoclave was cooled to room temperature naturally, the rosy products were collected by filtration, rinsed several times with deionized water and absolute ethyl alcohol, and dried at 60 °C. Finally, the Co_3O_4 nanocrystals were obtained by thermal decomposition of the rosy precursor at 350 °C and 500 °C for 2 h in air, respectively.

* Corresponding author. Tel.: +86 551 5591453; fax: +86 551 5591434.
E-mail address: gtfei@issp.ac.cn (G.T. Fei).

0169-4332/$ – see front matter © 2011 Elsevier B.V. All rights reserved.
doi:10.1016/j.apsusc.2011.02.066

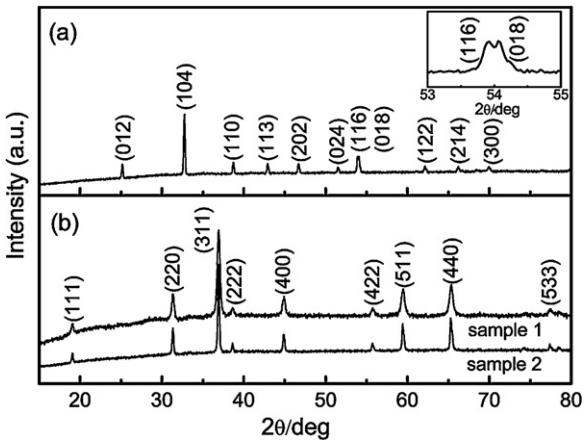

Fig. 1. XRD patterns of the (a) rosy precursor $CoCO_3$ and (b) Co_3O_4 annealed at 350 °C and 500 °C, corresponding to the label of sample 1and sample 2, respectively.

2.2. Characterization

The samples were characterized by X-ray powder diffraction (XRD, Philips X'pert PRO diffractometer, Cu Kα radiation), field emission scanning electron microscopy (FESEM, Hitachi S-4800) and high-resolution transmission electron microscopy (HRTEM, JEOL, 2010)

2.3. Photocatalytic activities measurement

50 ml of 20 mg/L reactive black (Yangzhou chemicals Co. Yangzhou China) solution were used for the photocatalytic experiment. The pH value of the solution was adjusted to 11 with KOH. 30 mg of the Co_3O_4 powder were added to reactive black solution and stirred with a magnetic stirrer in the dark room for 30 min to establish adsorption equilibrium between the solution and catalysts before exposures to the irradiation from the 500 W Mercury Lamp (Bylabo, Xi'an China). After certain time intervals, 2 ml reactive dye aqueous solution was taken out from the reactor vessel and centrifuged to separate the solution and the suspended catalysts. The UV–vis adsorption spectrums of the filtered solution were measured using a spectrophotometer (Cary 500), and the concentration of the reactive dye aqueous solution was estimated by the value of the adsorption peaks. All the experiments were performed at room temperature.

3. Results and discussion

3.1. Structural characterization

The X-ray diffraction (XRD) pattern of the as-prepared rosy precursor is shown in Fig. 1a. All the diffraction peaks can be indexed as rhombohedral $CoCO_3$ (JCPDS 78-0209, $a = 4.6618$ Å, $c = 14.9630$ Å). After annealing in air at high temperature, the precursors would be oxidized, and Co_3O_4 products can be obtained in accordance with the chemical reaction equation

$$6CoCO_3 + O_2 \rightarrow 2Co_3O_4 + 6CO_2$$

where the CO_2 vaporizes. Fig. 1b presents the XRD patterns of the sample 1 and sample 2, which were obtained after annealing the rosy precursor in air at 350 °C and 500 °C for 2 h, respectively. It can be seen that all the diffraction peaks agree well with the cubic Co_3O_4 (JCPDS 76-1802, $a = 8.072$ Å). No other peaks have been detected, indicting that the products are of high purity. According to Scherrer's formula, the crystalline size, determined from the strongest peak located at about 37°, is calculated to be only 14 nm for sample 1, and 34 nm for sample 2. The increase in crystalline size of the sample 2 can be ascribed to the agglomeration and ripening of the small crystallite during calcination process at high temperature [24].

The FESEM images of the products are shown in Fig. 2. The as-prepared $CoCO_3$ products with the diameter approximate 5–7 μm are of urchin-like microstructures, which are built of many nanowires with the smooth surface (Fig. 2a). Enlarger observation shown in Fig. 2b indicates that these radial nanowires are of several nanometers in diameter. The images of sample 1 and sample 2, calcined at 350 °C and 500 °C for 2 h, respectively, are shown in Fig. 2c–f. As seen in Fig. 2c and e, the overall morphology of the sample 1 and sample 2 are still of urchin-like microstructure, which retain the typical morphology of the precursors. FESEM images of sample 1 and sample 2 shown in Fig. 2d and f clearly show that those radial nanowires are converted to the radial particles chain after annealed in the air. These nanoparticles with the diameter of ca. 15 nm and 35 nm in average for sample 1 and sample 2, respectively, interconnect together and constitute the nanoparticle chain. The crystalline size estimated from the images is founded to be in good agreement with the XRD results.

3.2. Photocatalytic measurement.

The photocatalytic activities of the hierarchical micro/nanostructures Co_3O_4 in the degradation of the reactive black was shown in Fig. 3. Fig. 3a depicts the UV–vis absorption spectra of the reactive black aqueous solution with 30 mg urchin-like Co_3O_4 of sample 1 after exposure to the UV-light for different duration. It can be seen that the characteristic absorption peak of the reactive black at ca. 615 nm decreased evidently after irradiation for 70 min. In order to demonstrate the distinction of the photocatalytic activity of the sample 1 and sample 2, the identical experiment was also performed for the catalyst of sample 2 as it did to sample 1. Fig. 3b represents the variation of the relative concentration of the remaining dyes in solution versus the irradiation time from the optical absorbance measurements at ca. 615 nm. Without any irradiation from the UV light, the concentration of the reactive dye aqueous solution decreased quite a little, about 10% or less (curve 1), while without any catalyst, the concentration of the reactive dye aqueous solution was reduced by almost 40% in 70 min (curve 2). With addition of the catalysts of Co_3O_4, the degradation efficiency could be enhanced, which reached to approximately 82% and 51% for sample 1 and sample 2, respectively, corresponding to the curve 3 and curve 4. Obviously, sample 1 has much higher photocatalysis efficiency for reactive black than sample 2, which results from its much larger specific surface area.

On the basis of the concept of the AOPs technology mentioned above, we presume the photocatalytic processes of the urchin-like Co_3O_4 are probably result from two ways, one is the direct oxidation of the reactive dye by the holes generated by the UV irradiation and the other is the degradation by hydroxyl radical (•OH), an extremely strong and no-selective oxidant [1,5]. At first, the electron–hole pairs formed on the surface of the semiconductor Co_3O_4 by the irradiation of the UV light, similar to the photocatalytic activities of ZnO and TiO_2 [25–27]. Then the holes with the high oxidative potential either direct oxidize the reactive dye or react with the OH^- to form hydroxyl radical (•OH). The total reaction between the Co_3O_4 and the reactive dye could be written as follows [1].

$$(Co_3O_4) + h\nu \rightarrow (Co_3O_4)(e^-_{CB} + h^+_{VB}) \quad (1)$$

$$h^+_{VB} + \text{dye} \rightarrow \text{dye}^{\bullet+}(\text{oxidation of the dye}) \quad (2)$$

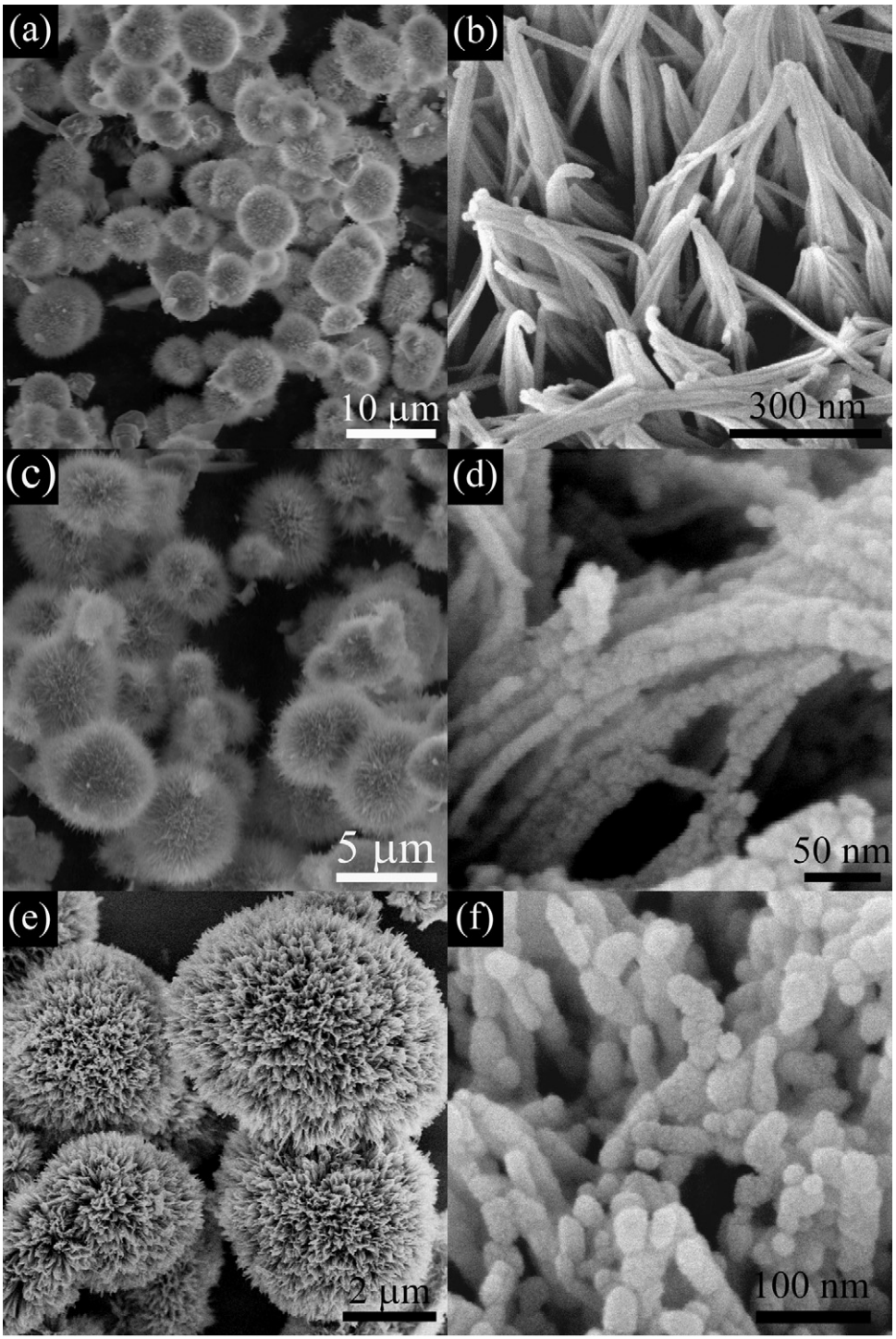

Fig. 2. (a and b) Low and high magnification SEM images of precursor. (c and d) Low and high magnification SEM images of sample 1. (e and f) Low and high magnification SEM images of sample 2.

or

$$h^{+}_{VB} + OH^{-} \rightarrow {}^{\bullet}OH \quad (3)$$

$${}^{\bullet}OH + \text{dye} \rightarrow \text{degradation of the dye} \quad (4)$$

It is well known that the degradation efficiency strongly depends on the specific surface area of catalysts, as the electron–hole pairs are usually generated on the surface of the catalysts [28,29]. The larger the specific surface area was, the more holes generated on the surface and the more reactive sites formed for the reactive dye, which could promote the degradation efficiency markedly. As to our photocatalytic system, sample 1 presents the better degradation efficiency due to its larger specific surface area than that of sample 2. The results are in coinciding with our analysis and further proved our presumption is plausibly.

The circled photocatalytic degradation of sample l is also studied. After each run, the catalysts were collected and washed with the deionized water for several times. The catalyst is reused under the same conditions as the first run, and its photocatalytic activities is almost the same to that of the first run, as seen in Fig. 4,

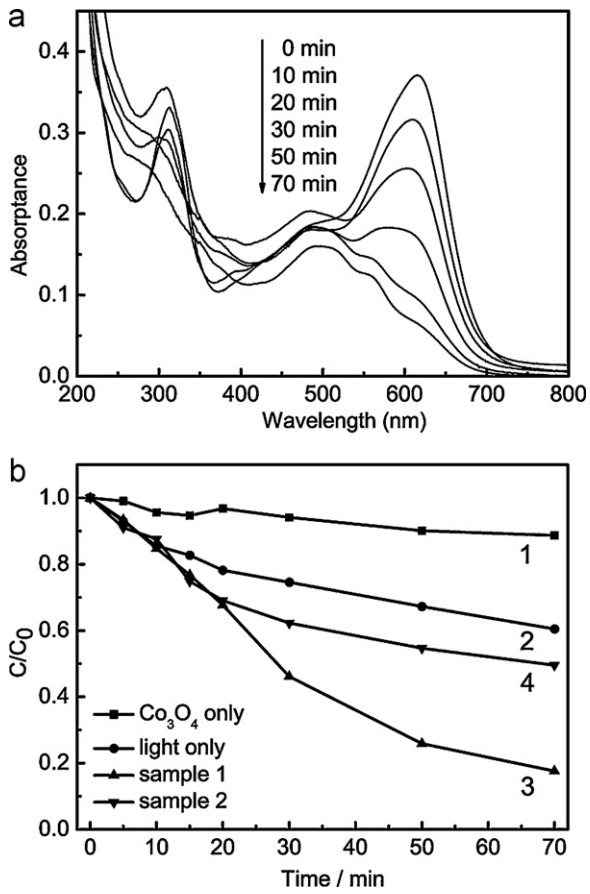

Fig. 3. Photocatalytic degradation studies of Co_3O_4. (a) Evolution of UV–vis absorption spectrum of reactive black during the photocatalytic degradation at different time of sample 1. (b) Photocatalytic efficiency (C/C_0) of reactive black dye solution versus irradiation time. (1) Without UV light irradiation, (2) Without any catalysts, (3) 30 mg catalysts of sample 1, (4) 30 mg catalysts of sample 2.

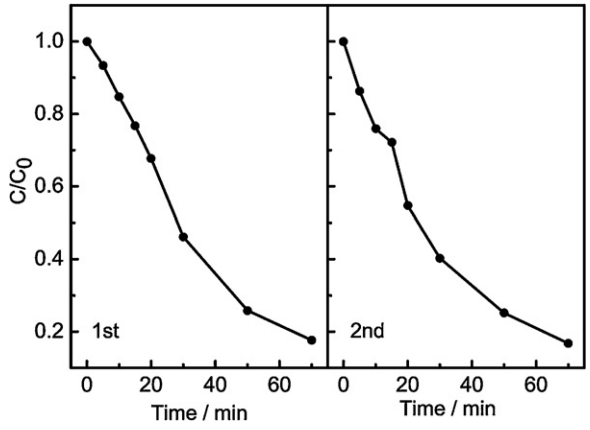

Fig. 4. Recycled degradation data of reactive black dye solution using Co_3O_4 catalysts of sample 1.

which demonstrates the good stability of Co_3O_4. Results indicate that the prepared Co_3O_4 has a good prospect on the purification of the waste water polluted by the reactive dye.

4. Conclusion

The urchin-like Co_3O_4 were successfully synthesized through a simple hydrothermal process and subsequently calcination. These urchin-like Co_3O_4 products with the diameter of ca. 5-7 μm were composed of numerous nanoparticles. Photocatalytic measurement demonstrated that the as-synthesized Co_3O_4 displays good degradation efficiency for the reactive dye, and the degradation efficiency significantly depends on their specific surface area. The reaction mechanism was also proposed, which is ascribed to the photogenerated electron–hole pairs on the surface of Co_3O_4. Furthermore, the as-synthesized Co_3O_4 with unique structural and small particle size would also exhibit a great potential application in the catalysts, lithium ion batteries, sensors and other applications.

Acknowledgments

This work was supported by the National Natural Science Foundation of China (no. 11074254), the Ministry of Science and Technology of China (no. 2005CB623603), Hundred Talent Program of Chinese Academy of Sciences, and the President Foundation of Hefei Institute of Physical Sciences, Chinese Academy of Sciences.

References

[1] S.K. Kansal, N. Kaur, S. Singh, Nanoscale Res. Lett. 4 (2009) 709.
[2] Z. Aksu, Process Biochem. 40 (2005) 997.
[3] J. Fernandez, J. Bandara, A. Lopez, P. Buffat, J. Kiwi, Langmuir 15 (1999) 185.
[4] J. Madhavan, P. Maruthamuthu, S. Murugesan, M. Ashokkumar, Appl. Catal. A: Gen. 368 (2009) 35.
[5] V. Sarria, S. Parra, N. Adler, P. Peringer, N. Benitez, C. Pulgarin, Catal. Today 76 (2002) 301.
[6] J.H. Pan, H.Q. Dou, Z.G. Xiong, C. Xu, J.Z. Ma, X.S. Zhao, J. Mater. Chem. 20 (2010) 4512.
[7] P. Raja, M. Bensimon, U. Klehm, P. Albers, D. Laub, L. Minsker-Kiwi, A. Renken, J. Kiwi, J. Photochem. Photobiol. A 187 (2007) 332.
[8] Z.Y. Yu, M. Bensimon, D. Laub, L. Kiwi-Minsker, W. Jardim, E. Mielczarski, J. Mielczarski, J. Kiwi, J. Mol. Catal. A 272 (2007) 11.
[9] A.M. Cao, J.S. Hu, H.P. Liang, W.G. Song, L.J. Wan, X.L. He, X.G. Gao, S.H. Xia, J. Phys. Chem. B 110 (2006) 15858.
[10] K.I. Choi, H.R. Kim, K.M. Kim, D.W. Li, G.Z. Cao, J.H. Lee, Sens. Actuator B: Chem. 146 (2010) 183.
[11] W.Y. Li, L.N. Xu, J. Chen, Adv. Funct. Mater. 15 (2005) 851.
[12] D. Barreca, M. Cruz-Yusta, A. Gasparotto, C. Maccato, J. Morales, A. Pozza, C. Sada, L. Sanchez, E. Tondello, J. Phys. Chem. C 114 (2010) 10054.
[13] B. Guo, C.S. Li, Z.Y. Yuan, J. Phys. Chem. C 114 (2010) 12805.
[14] P. Poizot, S. Laruelle, S. Grugeon, L. Dupont, J.M. Tarascon, Nature 407 (2000) 496.
[15] W.L. Yao, J. Yang, J.L. Wang, Y. Nuli, J. Electrochem. Soc. 155 (2008) A903.
[16] L.H. Hu, Q. Peng, Y.D. Li, J. Am. Chem. Soc. 130 (2008) 16136.
[17] L.H. Hu, K.Q. Sun, Q. Peng, B.Q. Xu, Y.D. Li, Nano Res. 3 (2010) 363.
[18] X.W. Xie, Y. Li, Z.Q. Liu, M. Haruta, W.J. Shen, Nature 458 (2009) 746.
[19] J. Ryu, S.W. Kim, K. Kang, C.B. Park, ACS Nano 4 (2010) 159.
[20] S.G. Kandalkar, C.D. Lokhande, R.S. Mane, S.H. Han, Appl. Surf. Sci. 253 (2007) 3952.
[21] M.M. Rahman, J.Z. Wang, X.L. Deng, Y. Li, H.K. Liu, Electrochim. Acta 55 (2009) 504.
[22] A. Askarinejad, M. Bagherzadeh, A. Morsali, Appl. Surf. Sci. 256 (2010) 6678.
[23] D. Patil, P. Patil, V. Subramanian, P.A. Joy, H.S. Potdar, Talanta 81 (2010) 37.
[24] J. Zheng, J. Liu, D.P. Lv, Q. Kuang, Z.Y. Jiang, Z.X. Xie, R.B. Huang, L.S. Zheng, J. Solid State Chem. 183 (2010) 600.
[25] G. Williams, B. Seger, P.V. Kamat, ACS Nano 2 (2008) 1487.
[26] C.G. Tian, W. Li, K. Pan, Q. Zhang, G.H. Tian, W. Zhou, H.G. Fu, J. Solid State Chem. 183 (2010) 2720.
[27] K.H. Ji, D.M. Jang, Y.J. Cho, Y. Myung, H.S. Kim, Y. Kim, J. Park, J. Phys. Chem. C 113 (2009) 19966.
[28] F. Lu, W. Cai, Y. Zhang, Adv. Funct. Mater. 18 (2008) 1047.
[29] M. Wang, G.T. Fei, L.D. Zhang, Nanoscale Res. Lett. 5 (2010) 1800.